Article:
Papadimitriou, I, Utton, C, Scott, A et al. (1 more author) (2015) Ab Initio Study of Binary and Ternary $Nb_3(X,Y)$ A15 Intermetallic Phases (X,Y = Al, Ge, Si, Sn). Metallurgical and Materials Transactions A, 46 (2). 566 - 576. ISSN 1073-5623

https://doi.org/10.1007/s11661-014-2403-1

Ab initio study of binary and ternary $Nb_3(X,Y)$ A15 intermetallic phases (X,Y= Al, Ge, Si, Sn)

I. Papadimitriou[a], C. Utton[a], A. Scott[b], P. Tsakiropoulos[a]

[a] Department of Materials Science and Engineering, The University of Sheffield, Sir Robert Hadfield Building, Mappin Street, Sheffield S1 3JD, England, UK

[b] Institute for Materials Research, The University of Leeds, Leeds LS2 9JT, England, UK

Abstract

Elastic and thermodynamic properties of binary and ternary A15 phases containing Al, Ge, Si and Sn were studied using the first-principles pseudopotential plane-wave method based on density functional theory. The temperature dependence of the enthalpy of formation for the A15 intermetallics is reported using the quasiharmonic approximation. Elastic properties of the studied compounds were calculated at T = 0 K and were in agreement with the measured values reported in the literature. The elastic properties and thermodynamic data for the metastable A15-Nb_3Si are reported for the first time. The Nb_3Si has the highest bulk, shear and Young's modulus values and is predicted to be less ductile than the other three binary A15 intermetallics. The calculations suggest (i) that Al and Sn have a positive effect on the ductility of the A15 compounds of this study, (ii) that Ge as a ternary addition has a ductilizing effect only in the A15-Nb_3Si, and (iii) that Si as a ternary addition has a negative effect on the ductility of all the A15 compounds of the present study. The linear thermal expansion coefficients of the Nb, Al, the A15 Nb_3Al, Nb_3Ge, Nb_3Sn and Nb_3Si (A15) phases are reported. The Sn and Al additions in the Nb_3Si stabilise the A15 structure, while the Ge addition has the opposite effect, stabilising the *tP*32 Nb_3Si.

* Corresponding author: p.tsakiropoulos@sheffield.ac.uk, fax +440(0)1142225943

Paper presented at the Symposium "Materials for High-Temperature Applications: Next generation Superalloys and Beyond" at TMS Annual 2014.

1. Introduction

High-temperature structural materials with operating temperature capability that exceeds that of modern Ni-based superalloys are currently developed to meet environmental and performance targets for future gas turbine engines. Alloys based on refractory metal intermetallic compounds can achieve a balance of mechanical and environmental properties with low density and thus are considered as candidate materials. The microstructures of these materials can contain intermetallics with the A15 cubic structure [1, 2].

Niobium silicide based alloys have attracted much interest as the next generation ultra-high temperature alloys owing to their creep, high temperature strength and ambient temperature fracture toughness [3, 4]. Their microstructures consist of an Nb solid solution phase in which are embedded silicide(s) and other intermetallic phase(s) or vice versa, depending on alloy composition [3-5]. The choice of the latter is influenced by considerations about achieving a balance of high and ambient temperature properties [1, 3, 4].

The Nb_3Si and Nb_5Si_3 silicides can be present in the microstructure of Nb silicide based alloys [3, 4]. Both silicides can form as stable and metastable compounds [6]. In the Nb-Si binary phase diagram the equilibrium (stable) 5-3 silicide has the βNb_5Si_3 tetragonal structure at high temperatures and the αNb_5Si_3 tetragonal structure at low temperatures and the tetragonal (stable) Nb_3Si transforms via a eutectoid reaction to Nb_{ss} and αNb_5Si_3 [6] which can be used to generate desirable microstructures in the alloys [3]. Metastable Nb_3Si can form with the A15 cubic structure. There is no data about phase transformations involving the A15-Nb_3Si.

Additions of Al, Ge and Sn in Nb-18Si (at.%) alloys have been shown to benefit their oxidation behaviour [5, 7-9] and to influence the transformation of βNb_5Si_3 to αNb_5Si_3 [4]. These elements suppress the formation of the tetragonal (stable) Nb_3Si [10-12] and Sn plays a key role in the elimination of pest oxidation [5, 9]. The effectiveness of Sn depends on its concentration and its synergy with other elements in the alloy and on whether the A15-Nb_3Sn is stable in the microstructure. Furthermore, Sn can stabilise metastable forms of the Nb_3Si when it is in synergy with Fe and Cr [13]. The formation of A15-Nb_3Al in Nb silicide based alloys is possible depending on the Ti/Al ratio in the alloy [14].

In the equilibrium Nb-Si binary phase diagram the Nb_3Si has a tetragonal Ti_3P-type crystal structure. In Nb-Si-Ti based alloys the formation of the A15 Nb_3Sn destabilises the tetragonal Nb_3Si [10]. Some intermetallic phases with the A15 cubic structure have also attracted interest because of their superconducting properties. Niobium forms a number of superconducting A15 compounds that exhibit high transition temperatures (T_c), namely Nb_3Ge (23.6 K), Nb_3Ga (20.2 K), Nb_3Sn (18.9 K) and Nb_3Al (18.8 K). It has been suggested that the A15 Nb_3Si phase would have a T_c above that of Nb_3Ge, of the order of 25 K [15], owing to its small lattice parameter.

The A15 structure is a close-packed structure whose stability is largely governed by size [15]. It has a primitive cell of 8 atoms and belongs to the space group O^3_h - P*m*3*n*, its Pearson symbol is *cP*8 and is of the Cr_3Si type. The A_3B cubic unit cell has two B atoms at (0, 0, 0) and (0.5, 0.5, 0.5) sites and six A atoms at (0.25, 0, 0.5), (0.5, 0.25, 0), (0, 0.5, 0.25), (0.75, 0, 0.5), (0.5, 0.75, 0) and (0, 0.5, 0.75) sites. In the current study the A atoms are Nb while the B atoms are Sn, Al, Ge or Si. In the case of the

ternary compounds, two different atoms occupy either the (0, 0, 0) or (0.5, 0.5, 0.5) sites.

The resistivity [16, 17], heat capacity [18, 19], electron-phonon interaction [20] and magnetic susceptibility [21] of A15 compounds have been studied. There is limited data about enthalpies of formation and Debye temperature of the A15-Nb_3X (X=Sn, Al, Si, Ge) compounds [18-19]. The elastic properties of Nb_3Sn and Nb_3Al have been calculated [22, 23], but to the best of the authors' knowledge no data exists for the A15 Nb_3Si and Nb_3Ge intermetallics. There is experimental and theoretical data for the vibrational and elastic properties of Nb, Si, Sn, Ge and Al [24, 25] and their Debye temperatures [26]. There is also experimental data for the linear thermal expansion coefficients of Nb, Al and Nb_3Ge [25, 27, 28].

The motivation for the present study was to investigate the elastic and thermodynamical properties of binary and ternary A15 Nb based intermetallics and to compare the stability of A15-Nb_3Si with the tP32-Nb_3Si. Calculations of the elastic constants and phonon properties are used to produce a complete set of data for the studied intermetallics. This data will be used to support the design of Nb silicide based alloys.

2. Computational details

2.1 Methodology

The calculations were performed using the CASTEP (Cambridge Serial Total Energy Package) code [29]. The Kohn–Sham approach was used to calculate the fundamental eigenvalues [30]. The interaction between valence electrons and core electrons was treated under the pseudopotential approximation and the plane-wave

approach [31]. The exchange-correlation energy was evaluated with the help of the generalised gradient approximation (Perdew–Wang, PW91) [32]. To reduce the basis set of plane wave functions used to describe the real electronic functions, norm conserving pseudopotentials [33] were implemented and the valences for the atomic configurations were Al-$3s^2 3p^1$, Sn-$5s^2 5p^2$, Nb-$4d^4 5s^1$, Ge-$4s^2 5p^2$ and Si-$3s^2 3p^2$. After conducting careful convergence tests it was found that an energy cutoff of 700 eV was sufficient to reduce the error in the total energy to less than 0.1 meV/atom. A Monkhorst–Pack k-point grid separation of 0.03 $Å^{-1}$ was employed for the integration over the Brillouin zone according to the Monkhorst–Pack scheme [34]. A well converged k-point set was needed to calculate high quality thermodynamic properties; thus separate convergence tests were carried out to ensure that the error in the phonon frequencies was less than 10^{-3} cm^{-1}. A finite basis set correction and the Pulay scheme of density mixing were applied for the evaluation of energy and stress, while the electronic energy tolerance for the SCF solver was 1×10^{-10} eV. Geometry optimisations of the structures were performed within the Broyden-Fletcher-Goldfarb-Shanno (BFGS) minimization scheme [35] , with the following thresholds for converged structures: energy change per atom, maximum residual force, maximum atomic displacement and maximum stress less than 1×10^{-7} eV, 1×10^{-4} eV/Å, 1×10^{-4} Å and 0.001 GPa, respectively.

2.2 Elastic properties

The elastic constants of a material describe its response to an applied stress, or the stress required to maintain a distortion. The method to determine elastic constants consisted of applying a given strain and calculating the stress, since the unit cell was kept fixed and only the internal coordinates were optimised. Both stress and strain have three tensile and three shear components, giving six in total. The linear elastic

constants form a 6 x 6 matrix such that $\sigma_i=C_{ij}\varepsilon_j$ for small stress σ and strain ε. This matrix can be reduced as the strain patterns (sets of distortions) are based on the crystal structure of each phase which means that one pattern is sufficient for cubic cells by taking advantage of the linear combinations of the second order elastic constants. Six strain steps (varying from -0.003 to + 0.003) were used for each pattern to obtain a consistent linear fit of the stress-strain relationship.

Thus, for the cubic binary and ternary A15 compounds of this study, and the bcc (Nb), diamond (Si) and fcc (Al) structures a series of six geometry optimisations were conducted in order to evaluate the three independent elastic constants C_{11}, C_{12} and C_{44}. For the tetragonal Sn 12 geometry optimisations were required to calculate the six independent elastic constants C_{11}, C_{12}, C_{13}, C_{33}, C_{44} and C_{66}. After acquiring the elastic constants matrix and confirming that the mechanical stability criteria [36] are satisfied, the bulk (B), Young's (E) and shear (G) modulus and Poisson's ratio (v) were obtained by using the Voigt-Reuss-Hill approximation (VRH) [37, 38]. The Debye temperature at low temperatures was determined from elastic constants using the equations in [39], since at low temperatures the vibrational excitations arise solely from acoustic modes, i.e. when the Debye temperature is associated with lattice vibrations. In order to confirm the values of the bulk moduli, a fit of the energies versus the volumes of the strained structures in the third order Birch-Murnaghan equation of state (B-M EOS) [40] was carried out.

2.3 Linear Response method

The entropic contributions play a predominant role in the structural stability of intermetallic phases. In the case of strongly ordered compounds the main contribution comes from the vibrational entropy, as the electronic and configurationally entropies

are considered to be relatively small [41]. Density Functional Perturbation Theory (DFPT) or Linear Response, which is one of the most popular methods of lattice dynamics [42-43], was used in order to obtain the vibrational density of states. When ionic positions are perturbed, the dynamical matrix and phonon frequencies can be obtained. The calculations first ensured that every system was in the ground state, i.e., the geometry optimisation was fully converged as any underconverged structure could yield imaginary phonon frequency eigenvalues, which is indicative of mechanical instability. After directly computing the phonon frequencies on Monkhorst-Pack q-vector grid of separation of 0.05 $Å^{-1}$, the results were interpolated onto a very dense q-point set, thus the phonon density of states (DOS) was obtained for each phase under investigation. By using the phonon DOS and the formulae in [42], the vibrational contributions to the enthalpy, entropy and free energy versus temperature as well as the Debye temperature were obtained using the quasiharmonic approximation. Apart from the A15 compounds that were under study, the phonon DOS of each element were also calculated separately in order to obtain the finite temperature enthalpy of formation.

The linear thermal expansion coefficients were obtained by generating structures by varying the ratio V/V_0 (V_0 being the equilibrium volume at 0 K) from 0.991 to 1.006 with an increment of 0.003 and conducting a phonon calculation for each volume. The equilibrium volume V(T,P) was then calculated at every given temperature using the quasiharmonic approximation by minimising the total free energy with respect to volume, thus finding the equilibrium volume at each temperature. After calculating the V(T,P) the linear thermal expansion coefficient was obtained. This procedure was repeated for Nb, Al, Nb_3Sn, Nb_3Al, Nb_3Ge and the A15 Nb_3Si.

3. Results and discussion

The calculated lattice constants of the pure elements and the binary and ternary A15 phases are compared with the experimental ones in Table 1. It can be seen that in the present calculations and with the exception of Si and Ge the lattice constants are slightly underestimated but overall are in good agreement with the experimental values, with the lattice constant of Al showing the largest difference of 1.85 %. Table 2 gives the results for the independent elastic constants (C_{ij}) and bulk moduli (B) for all elements and compounds under study. In this Table the bulk moduli were calculated from elastic constants according to the Voigt-Reuss-Hill (VRH) scheme and values are also given for bulk moduli and first pressure derivatives of bulk moduli (B') from the Birch-Murnaghan equation of state (B-M EOS). It is confirmed that the mechanical stability criteria [36] are met for all phases. For the pure elements it can be seen that the elastic constants are in good agreement with the experimental data. The values of the bulk moduli of the Nb_3Sn and Nb_3Al are in good agreement with other theoretical [22, 23] results and the consistency of the calculation is validated by the results of the B-M EOS fitting. The current results show that the Nb_3Si has the highest bulk modulus of 181.5 GPa and that the bulk moduli of the Nb_3Sn and Nb_3Al are close to each other being 167.6 GPa and 162.2 GPa, respectively, while the corresponding value for Nb_3Ge is 174.2 GPa. This means that the most resistant to applied pressure of the four binary intermetallics of this study is the Nb_3Si. From the bulk modulus values of the ternary A15 phases it can be seen that the Si and Ge tend to increase the bulk modulus, while the Sn and Al have the opposite effect.

The calculated values of the shear (G) and Young's (E) modulus and the Debye temperature (Θ_D) are given in Table 3. The Nb_3Si phase has the highest shear modulus value and the shear modulus decreases from Nb_3Si (80.3 GPa) to Nb_3Ge

(73.5 GPa), to Nb_3Sn (65 GPa) to Nb_3Al (61.6 GPa), which means that the most resistant binary compound to reversible deformation upon shear strain is the Nb_3Si. The same ranking applies for the stiffness of the compounds as the elastic modulus (E) values are 210 GPa for Nb_3Si, 193.3 GPa for Nb_3Ge, 172.7 GPa for Nb_3Sn and 164 GPa for Nb_3Al. Based on the values of the aforementioned moduli for the ternary phases, it is suggested that the Si and Ge additions increase the moduli, while the Sn and Al decrease them.

Ductile or brittle behavior of a material can be deduced by taking into account the Cauchy pressure (C_{12} - C_{44} for cubic and C_{13}-C_{44} and C_{12}-C_{66} for tetragonal lattices) and Pugh's [44] index of ductility of shear modulus over bulk modulus ratio (G/B) and Poisson's ratio (v) [45, 46]. The values of the aforementioned properties are listed in Table 3. According to [47], for metallic bonding, a positive value of Cauchy pressure means ductile behavior and brittle if negative. The other two conditions point to brittle behavior when the G/B ratio is greater than 0.57 and the v is less than 0.26. Bearing that in mind, it can be seen from Table 3 that the Nb_3Si and Nb_3Al are the most and least brittle binary compounds, respectively, that the Sn and Al additions may improve ductility, and that the Si has the opposite effect.

The calculations predict that when Al is added as a ternary addition in the A15 compounds the bulk and shear moduli decrease, the shear over bulk modulus ratio decreases and the Poisson's ratio increases, and that Si as a ternary addition in the A15 compounds has the exact opposite effect. When Sn is added as a ternary addition in the Nb_3Al the bulk and the shear moduli decrease, the shear over bulk modulus ratio decreases and the Poisson's ratio increases, and the opposite is the effect of Sn as a ternary addition in the Nb_3Ge and Nb_3Si. As a ternary addition in Nb_3Si, the Ge decreases the bulk and shear moduli values and the shear over bulk modulus ratio and

increases the Poisson's ratio but has the opposite effect when added to the Nb_3Al and Nb_3Sn compounds. It is therefore suggested that Al and Sn have a ductilizing effect in the A15 compounds of the present study, that Ge as a ternary addition has a positive effect only on the ductility of A15-Nb_3Si, and that Si as a ternary addition has a negative effect on the ductility of all the A15 compounds in the present study .

Comparing the shear moduli, Young's moduli and Debye temperature values calculated from the elastic constants of the Nb_3Sn and Nb_3Al of this study with theoretical data in [22], it can be seen that there is disagreement, which in the case of Nb_3Al is 17%, 15% and 18% in G, E and Θ_D, respectively, due to the deviation between the shear elastic constant values of this study and [22] (the bulk modulus values (Table 2) are in good agreement). The Debye temperature of Nb_3Al calculated from the elastic constants in the present study is in very good agreement with the experimental results [26]. It can thus be suggested that as the Θ_D value of the present study is much closer to that in [26] than the value in [22] that the shear constant calculated in this study is closer to the actual value than in [22], owing possibly to the use of different pseudopotentials. The Θ_D value decreases from Nb_3Si (420 K) to Nb_3Ge (376 K) to Nb_3Al (374 K) to Nb_3Sn (336 K). When Si or Ge are added to the A15 structure the Debye temperature tends to increase. The aforementioned value tends to decrease in the presence of Sn and Al.

The vibrational density of states (DOS) for the elemental phases and A15 compounds under study were computed and all the eigenfrequencies were found to be real, hence it was confirmed that the compounds under investigation are mechanically stable. The phonon DOS are shown in Fig. 1. After inserting the computed phonon DOS in the relevant equations [42], the vibrational contribution to free energies per atom (F^{phon} (T)) was calculated and is presented for all elemental phases and

compounds in Fig. 2. It can be seen that the F^{phonon} decreases faster in the order Nb_3Si, Nb_3Al, Nb_3Ge, Nb_3Sn. In Fig. 3 the phonon contribution to the free energy of the ternary compounds is shown. It can be seen that it decreases faster in the order Nb_6AlSi, Nb_6GeSi, Nb_6SiSn, Nb_6GeAl, Nb_6AlSn, Nb_6GeSn. After taking F^{phon} into account, the phonon contribution to the enthalpy of formation (ΔH_f^{phon} (T)) was evaluated. The ΔH_f^{phon} (T) rises faster for Nb_3Sn, owing to the steep descent of the vibrational contribution to the free energy of Sn compared with the other elements, as it can be seen in Fig. 4. The ΔH_f^{phon} (T) of Nb_3Si on the other hand exhibits the smallest slope of the four curves, which is attributed to the behaviour of the F^{phon} (T) of Si, while the curves of Nb_3Al and Nb_3Ge are close to each other and have about half the slope of the corresponding value of Nb_3Sn. Regarding the ternary phases the ΔH_f^{phon} (T) increases faster in the order Nb_6AlSi, Nb_6GeSn, Nb_6GeAl, Nb_6SiSn, Nb_6AlSn, Nb_6GeSn. By taking into consideration the total internal energies of the constituent elements and the compounds, the enthalpies of formation versus temperature (ΔH_f (T)) were obtained and they are shown in Figs 5 and 6. At T = 0 K the heat of formation (ΔH_f^0) increases from Nb_3Si (-34.734 kJ/mol) to Nb_3Ge (-33.288 kJ/mol), to Nb_3Al (-22.06 kJ/mol) to Nb_3Sn (-16.54 kJ/mole). Table 4 shows the good agreement between the present study and previous experimental and theoretical results regarding the enthalpies of formation of the intermetallics. It can be seen that there is agreement of the enthalpy of formation of the tP32-Nb_3Si with previous ab initio calculation [62] and values from CALPHAD assessments [63]. The Nb_3Si phase has the lowest ΔH_f (T) of the binary A15 intermetallics, while the Nb_3Sn is the phase with the highest value in the whole range of temperatures. The ΔH_f(T) of the tP32 Nb_3Si [48] is also shown in Fig. 4 and Table 4. It is confirmed that the tetragonal Nb_3Si is more stable than the cubic Nb_3Si. Even though the phonon contribution in

the enthalpy of formation of the *tP*32 Nb_3Si exhibits a steeper ascent than that of the A15 Nb_3Si, in the whole range of temperatures the enthalpy of formation of the former structure is always lower than that of the latter, owing mostly to the considerably lower enthalpy of formation at T = 0 K. For the ternary intermetallics containing Si and Sn, Al or Ge the enthalpy of formation at T = 0 K was calculated for the A15 and *tP*32 structures and the values are given in Table 4. It is suggested that the Sn and Al additions stabilise the A15 structure and the Ge addition stabilises the *tP*32 structure.

The linear thermal expansion coefficients of Nb, Al, Nb_3Sn, Nb_3Al, Nb_3Ge and Nb_3Si (A15) phases are shown in Table 5. The agreement with the available experimental data is excellent, a fact that demonstrates the power and usefulness of the linear response method. Regarding the A15 phases the aforementioned value tends to decrease in the order Nb_3Si (8.1 10^{-6}/K), Nb_3Ge (7.6 10^{-6}/K), Nb_3Al (7 10^{-6}/K), Nb_3Sn (6.4 10^{-6}/K).

The resultant phonon DOS from the calculations was also used to calculate the Debye temperature. It should be noted that it is more difficult to obtain accurate values of Θ_D in that way than through the elastic constants (see section 2.2) because Θ_D, as a low temperature property, is determined by low energy phonons i.e. the acoustic phonons. The lower the temperature the smaller the part of Brillouin Zone that contributes to thermodynamics. Despite this and although the values regarding the Nb_3Sn and Nb_3Al are somewhat underestimated, the calculated Θ_D values (Table 3) were in good agreement with both the experimental data [26] and the results of the present study that were calculated from elastic constants values. For the elemental phases the results were in good agreement with the literature. The overall correlation validates the quality of the calculations.

4. Conclusions

First-principles calculations were carried out for binary and ternary A15 intermetallic compounds and their constituent elements. Elastic constants, the bulk, shear and Young's moduli, the Poisson's ratio and the Debye temperature were calculated. In the case of the Nb_3Si, most of the data were obtained for the first time. The temperature dependence of the enthalpy of formation of the intermetallic phases is reported for the first time. The linear thermal expansion coefficients of Nb, Al, Nb_3Sn, Nb_3Al, Nb_3Ge and Nb_3Si (A15) are also reported. Comparison with available experimental and other theoretical data shows good agreement with this work. It is concluded that the A15 Nb_3Si has the highest bulk, shear and Young's modulus values and that it is the stiffest and less ductile of the four binary intermetallics of the present study. Among the binary A15 compounds the Θ_D value of Nb_3Si is the highest compared with the Nb_3Ge, Nb_3Sn and Nb_3Al compounds, while the ternary A15-Nb_6SiGe has the highest Θ_D value amongst the ternary intermetallics. It is suggested that Al and Sn additions in the ternary A15 compounds improve ductility. The results for the enthalpy of formation would suggest that the Sn and Al additions in the Nb_3Si stabilise the A15 structure rather than the *tP*32, and that the Ge addition in the Nb_3Si has the opposite effect.

Acknowledgements

The support of this work by the F-P7 "Accelerated Metallurgy" project and the EPSRC-Rolls Royce research partnership is gratefully acknowledged.

References

1. D. M. Shah, D. L. Anton, D. P. Pope and S. Chin, *Materials Science Engineering* 1995, vol. A192/193 pp. 658-672.
2. E. Passa, G. Shao and P. Tsakiropoulos, *Philosophical Magazine A* 1997, vol. 75, pp. 637-655.
3. S. J. Balsone, B. P. Bewlay, M. R. Jackson, P. R. Subramanian, J. C. Zhao, A. Chatterjee and T. M. Heffernan, In *Structural Intermetallics 2001*, ed. K. J. Hemker, Dimiduk D. M., Clemens H., Darolia R., Inui M., Larsen J. M., Sikka V. K., Thomas . and Whittenberger J. D. (TMS, Warrendale, 2001), pp 99-108.
4. P. Tsakiropoulos: *Beyond Nickel Based Superalloys.* In R. Blockley, W. Shyy (Eds) Encyclopedia of Aerospace Engineering, (John Wiley & Sons, Ltd, 2010), pp. 2345-2355.
5. J. Geng and P. Tsakiropoulos, *Intermetallics* 2007, vol. 15, pp. 382-395.
6. M.E. Schlesinger, H. Okamoto, A. B. Gokhale and R. Abbaschian, *Journal of Phase Equilibria* 1993, vol. 14, pp. 502-509.
7. J. Geng, P. Tsakiropoulos and G. Shao, *Materials Science and Engineering A* 2006, vol. 441, pp. 26-38.
8. K. Zelenitsas and P. Tsakiropoulos, *Materials Science and Engineering A-Structural Materials Properties Microstructure and Processing* 2006, vol. 416, pp. 269-280.
9. M. R. Jackson, B. P. Bewlay and J. C. Zhao, US patent 6,913,655 B2, (July 5, 2005).
10. N. Vellios and P. Tsakiropoulos, *Intermetallics* 2007, vol. 15, pp. 1518-1528.
11. K. Zelenitsas and P. Tsakiropoulos, *Intermetallics* 2006, vol. 14, pp. 639-659.
12. L. I. Zifu and P. Tsakiropoulos, *Intermetallics* 2010, vol. 18, pp. 1072-1078.
13. N. Vellios and P. Tsakiropoulos, *Intermetallics* 2007, vol. 15, pp. 1529-1537.
14. Yonosuke Murayama and Shuji Hanada, *Science and Technology of Advanced Materials* 2002, vol. 3, pp. 145-156.
15. D. Dew-Hughes, *Cryogenics* 1975, vol. 15, pp. 435-454.
16. D. W. Woodard and G. D. Cody, *Physical Review A-General Physics* 1964, vol. 136, pp. A166-168.
17. Z. Fisk and G. W. Webb, *Physical Review Letters* 1976, vol. 36, pp. 1084-1086.
18. G. S. Knapp, S. D. Bader and Z. Fisk, *Phys. Rev. B* 1976, vol. 13, pp. 3783-3789.
19. G. W. Webb, Z. Fisk, J. J. Engelhardt and S. D. Bader, *Phys. Rev. B* 1977, vol. 15, pp. 2624-2629.
20. B. M. Klein, L. L. Boyer and D. A. Papaconstantopoulos, *Physical Review Letters* 1979, vol. 42, pp. 530-533.
21. W. Rehwald, M. Rayl, R. W. Cohen and G. D. Cody, *Phys. Rev. B* 1972, vol. 6, pp. 363-371.
22. M. Sundareswari, Swaminathan Ramasubramanian and Mathrubutham Rajagopalan, *Solid State Communications* 2010, vol. 150, pp. 2057-2060.
23. C. Paduani, *Braz. J. Phys.* 2007, vol. 37, pp. 1073-1076.
24. W. A. Brantley, *J. Appl. Phys.* 1973, vol. 44, pp. 534-535.
25. C. J. Smithells: *Metal References Book*. (5th Edition Butterworth, London, 1976).
26. C. Kittel: *Introduction to Solid State Physics*. (7th edition John Wiley & Sons, New York, 1996).
27. Robert Grill and Alfred Gnadenberger, *Int. J. Refract. Met. Hard Mater.* 2006, vol. 24, pp. 275-282.
28. H. Kawamura, K. Tachikawa, K. Takemura and S. Minomura, *Journal of the Physical Society of Japan* 1979, vol. 47, pp. 1365-1366.
29. S. J. Clark, M. D. Segall, C. J. Pickard, P. J. Hasnip, M. J. Probert, K. Refson and M. C. Payne, *Z. Kristall.* 2005, vol. 220, pp. 567-570.
30. W. Kohn and L. J. Sham, *Physical Review* 1965, vol. 140, pp. 1133-1138.
31. M. C. Payne, M. P. Teter, D. C. Allan, T. A. Arias and J. D. Joannopoulos, *Rev. Mod. Phys.* 1992, vol. 64, pp. 1045-1097.

32. John P. Perdew, J. A. Chevary, S. H. Vosko, Koblar A. Jackson, Mark R. Pederson, D. J. Singh and Carlos Fiolhais, *Phys. Rev. B* 1992, vol. 46, pp. 6671-6687.
33. J. S. Lin, A. Qteish, M. C. Payne and V. Heine, *Phys. Rev. B* 1993, vol. 47, pp. 4174-4180.
34. Hendrik J. Monkhorst and James D. Pack, *Phys. Rev. B* 1976, vol. 13, pp. 5188-5192.
35. B. G. Pfrommer, M. Cote, S. G. Louie and M. L. Cohen, *J. Comput. Phys.* 1997, vol. 131, pp. 233-240.
36. M. Born and K. Huang: *Dynamical Theory of Crystal Lattices*. (Oxford, 1956).
37. R. Hill, *Proceedings of the Physical Society of London Section A* 1952, vol. 65, pp. 349-355.
38. A. Reuss, *Z. Angew. Math. Mech.* 1929, vol. 9, pp. 49-58.
39. O. L. Anderson, *Journal of Physics and Chemistry of Solids* 1963, vol. 24, pp. 909-917.
40. F. Birch, *Phys Rev* 1947, vol. 71, pp. 809-824.
41. Y. Wang, C. Woodward, S. H. Zhou, Z. K. Liu and L. Q. Chen, *Scripta Materialia* 2005, vol. 52, pp. 17-20.
42. Stefano Baroni, Stefano de Gironcoli, Andrea Dal Corso and Paolo Giannozzi, *Rev. Mod. Phys.* 2001, vol. 73, pp. 515-562.
43. S. De Gironcoli, *Phys. Rev. B* 1995, vol. 51, pp. 6773-6776.
44. S. F. Pugh, *Philosophical Magazine* 1954, vol. 45, pp. 823-843.
45. M. C. Gao, Y. Suzuki, H. Schweiger, O. N. Dogan, J. Hawk and M. Widom, *Journal of Physics-Condensed Matter* 2013, vol. 25.
46. M. C. Gao, O. N. Dogan, P. King, A. D. Rollett and M. Widom, *JOM* 2008, vol. 60, pp. 61-65.
47. D. G. Pettifor, *Mater. Sci. Technol.* 1992, vol. 8, pp. 345-349.
48. H. Nowotny, A. W. Searcy and J. E. Orr, *J. Phys. Chem.* 1956, vol. 60, pp. 677-678.
49. P. Soderlind, O. Eriksson, J. M. Wills and A. M. Boring, *Phys. Rev. B* 1993, vol. 48, pp. 5844-5851.
50. J. A. Rayne and B. S. Chandrasekhar, *Physical Review* 1960, vol. 120, pp. 1658-1663.
51. G. Simmons and H. Wang: *Single Crystal Elastic Constants and Calculated Aggregate Properties: A Handbook*. (1971).
52. C. Filippi, D. J. Singh and C. J. Umrigar, *Phys. Rev. B* 1994, vol. 50, pp. 14947-14951.
53. W. K. Wang, H. Iwasaki, C. Suryanarayana, T. Masumoto, N. Toyota, T. Fukase and F. Kogiku, *J. Mater. Sci.* 1982, vol. 17, pp. 1523-1532.
54. F. J. Bachner, J. B. Goodenough and H. C. Gatos, *Journal of Physics and Chemistry of Solids* 1967, vol. 28, pp. 889-895.
55. W. B. Pearson: *A Handbook of Lattice Spacings and Structures of Metals and Alloys*. (1967), pp. 978.
56. F. Galasso, B. Bayles and S. Soehle, *Nature* 1963, vol. 198, pp. 984.
57. K. Schubert: *in W. Koster (ed.), Kristallstrukturen Zweikomponentiger Phasen,*. (1964), pp. 305.
58. M. Arita, H. U. Nissen and W. Schauer, *J. Solid State Chem.* 1990, vol. 84, pp. 386-400.
59. C. Toffolon, C. Servant, J. C. Gachon and B. Sundman, *Journal of Phase Equilibria* 2002, vol. 23, pp. 134-139.
60. I. Shilo, H. F. Franzen and R. A. Schiffman, *Journal of the Electrochemical Society* 1982, vol. 129, pp. 1608-1613.
61. Kamal Mahdouk and Jean-Claude Gachon, *Journal of Alloys and Compounds* 2001, vol. 321, pp. 232-236.
62. Yue Chen, T. Hammerschmidt, D. G. Pettifor, Jia-Xiang Shang and Yue Zhang, *Acta Materialia* 2009, vol. 57, pp. 2657-2664.
63. G. Shao, *Intermetallics* 2004, vol. 12, pp. 655-664

Table 1

Lattice constants pure elements and binary and ternary A15 phases

Phase	this work (Å)	literature (Å)	deviation (%)
Nb	3.299	3.311 [a]	0.36
Sn	a=5.741 c=3.102	a=5.832 [b] c=3.182 [b]	Δa/a=1.56 Δc/c=1.37
Al	4.022	4.098 [c]	1.85
Si	5.469	5.431 [d]	0.70
Ge	5.738	5.658 [d]	1.41
Nb_3Sn	5.258	5.289 [e]	0.59
Nb_3Al	5.171	5.187 [e]	0.31
Nb_3Ge	5.151	5.168 [e]	0.33
Nb_3Si	5.101	5.155 [f]	1.05
Nb_6SnAl	5.221	5.255 [g]	0.65
Nb_6AlSi	5.136	5.173 [h]	0.72
Nb_6SnSi	5.186	5.216 [i]	0.58
Nb_6SnGe	5.21	5.217 [j]	0.13
Nb_6AlGe	5.161	5.175 [k]	0.27
Nb_6SiGe	5.126	5.173 [h]	0.91

[a] Ref [49], [b] Ref [50], [c] Ref [51], [d] Ref [52], [e] Ref [23], [f] Ref [53], [g] Ref [54], [h] Ref [55], [I] Ref [56], [j] Ref [57], [k] Ref [58]

Table 2

Elastic constants (C_{ij}) and bulk moduli (B) of pure elements and binary and ternary A15 phases in GPa.

	VRH approximation						B-M EOS		
Phase	C_{11}	C_{12}	C_{13}	C_{33}	C_{44}	C_{66}	B	B	B'
Nb	244	124.5			27		164.3	163.1	4.004
	253 [a]	133 [a]			31 [a]		170.3[a]		
Sn	74.2	58	22.2	81.2	23.4	9.9	51.8	53.2	3.703
	83.7 [b]	48.7 [b]	28.1 [b]	96.7 [b]	17.5 [b]	7.4 [b]	58 [b]		
Al	107.4	57.6			30.3		74.2	76.47	4.037
							75.2[a]		
Si	152.1	56.7			74.1		88.5	90.22	4.019
							98[c]		
Ge	113.9	40.5			55.2		65	67.5	4.035
	128.5 [c]	48.3 [c]			66.8 [c]		75[c]		
Nb_3Sn	282.4	110.1			53.8		167.6	167.5	4
							160.5[d]		
							166.5[e *]		
Nb_3Al	272.8	106.9			50.5		162.2	162.1	4
							156.3[d]		
							165.5[e *]		
Nb_3Ge	298.3	112.2			62.8		174.2	174	4
Nb_3Si	314.8	114.9			69.3		181.5	181.2	4
Nb_6SnAl	276.7	107.7			52		164	163.8	4
Nb_6AlSi	293.3	110.1			59.4		171.1	170.6	4
Nb_6SnSi	296.6	111.7			62		173.3	173	4
Nb_6SnGe	288.9	111.1			58.6		170.3	170	4
Nb_6AlGe	284.9	109.4			56.8		167.9	167.2	4
Nb_6SiGe	305.9	113.5			66.4		177.6	177	4

[a] Ref. [25] , [b] Ref [50], [c] Ref. [24], [d] Ref. [23], [e] Ref. [22], [*] calculated value

Table 3

Calculated shear (G) and elastic moduli (E) in GPa, Poisson's ratio (v), Cauchy pressure (C_{12}-C_{44} for cubic, C_{13}-C_{44} and C_{12}-C_{66} for tetragonal lattices) in GPa, G/B ratio and Debye temperature (Θ_D) from elastic constants for pure elements and binary and ternary A15 phases.

	G	E						Θ_D (K)			
Phase	VRH	VRH	v	C_{12}-C_{44}	C_{13}-C_{44}	C_{12}-C_{66}	G/B	Phonon DOS	Elastic constants		
Nb	37.4	104.3	0.394	97.5			0.228	277	268	275 [b]	
	37.5 [c]	104.9 [c]	0.397 [c]								
Sn	16.3	44.3	0.357	54.1	-1.2	48.1	0.315	254	217	230 [b]	
	18.4 [c]	49.9 [c]	0.357 [c]								
Al	28	74.7	0.334	27.3			0.377	394	420	428 [b]	
	26.2 [c]	70.6 [c]	0.345 [c]								
Si	62.1	151	0.216	-17.4			0.701	647	628	645 [b]	
	64.1 [d]	155.8 [d]	0.215 [d]								
Ge	46.9	113.4	0.209	-14.7			0.722	393	386	360 [b]	
	41 [d]	104 [d]									
Nb_3Sn	65	172.7	0.328	56.3			0.388	291	336	308 [b]	282 [a *]
	74.9 [a *]	195.3 [a *]									
Nb_3Al	61.6	164	0.331	56.4			0.380	353	374	370 [b]	316 [a *]
	74.2 [a *]	193.5 [a *]									
Nb_3Ge	73.5	193.3	0.315	49.4			0.422	344	376		
Nb_3Si	80.3	210	0.307	45.6			0.442	383	420		
Nb_6SnAl	63.2	168	0.329	55.7			0.385	332	355		
Nb_6AlSi	70.7	186.4	0.318	50.7			0.413	386	398		
Nb_6SnSi	72.8	191.6	0.316	49.7			0.420	360	378		
Nb_6SnGe	69.3	183.1	0.321	52.5			0.407	342	359		
Nb_6AlGe	67.6	178.8	0.323	52.6			0.403	350	377		
Nb_6SiGe	77	201.8	0.311	47.1			0.434	378	400		

[a] Ref. [22], [b] Ref. [26] [c] Ref. [25] , [d] Ref [24], [*] calculated value

Table 4

Calculated Enthalpies of formation of binary and ternary A15 phases (unless denoted otherwise) compared with the literature.

Phase	Temperature (K)	ΔH_f from the present study (kJ/mol)	Literature (kJ/mol)
Nb_3Sn	298	-15.583	-16.7 to -16 [a]
	1273	-11.36	-13.232 [a]
Nb_3Al	298	-22.061	-19.297 [b]
	1273	-20.07	-19.7 [c]
Nb_3Si	0	-34.734	-32.8 [d]
Nb_3Ge	0	-33.288	
Nb_6SnAl	0	-16.646	
Nb_6AlSi	0	-26.062	
Nb_6SnSi	0	-23.321	
Nb_6SnGe	0	-32.029	
Nb_6AlGe	0	-29.633	
Nb_6SiGe	0	-35.629	
Nb_3Si *tP*32	0	-37.3	-40.5 [d]
	298	-37	-29.6 to -35.9 [e]
Nb_6SiSn *tP*32	0	-15.985	
Nb_6SiAl *tP*32	0	-22.497	
Nb_6SiGe *tP*32	0	-36.021	

[a] Ref [59], [b] Ref [60], [c] Ref [61], [d] Ref [62], [e] Ref [63]

Table 5

Linear thermal expansion coefficients of Nb, Al, Nb_3Sn, Nb_3Al, Nb_3Ge and Nb_3Si (10^{-6}/K).

Phase	this work	literature
Nb *	7.9	7.3 [a]
Al *	22.5	23.1 [b]
Nb_3Sn	6.4	
Nb_3Al	7	
Nb_3Ge	7.6	7.7 [c]
Nb_3Si	8.1	

* At room temperature, [a] Ref [25], [b] Ref [27] , [c] Ref [28]

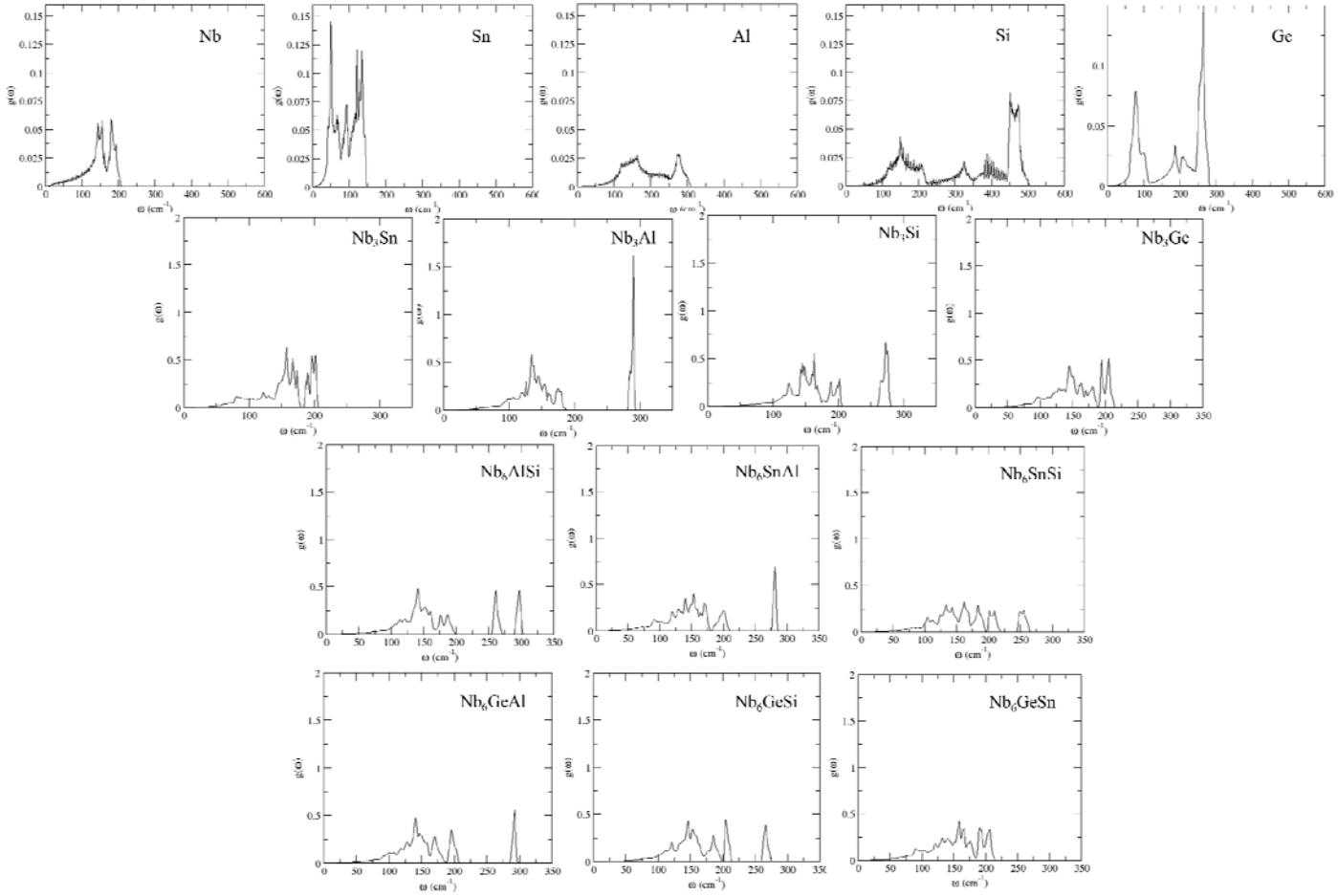

Fig. 1. Phonon DOS of the pure elements and the binary and ternary A15 intermetallics of the present study.

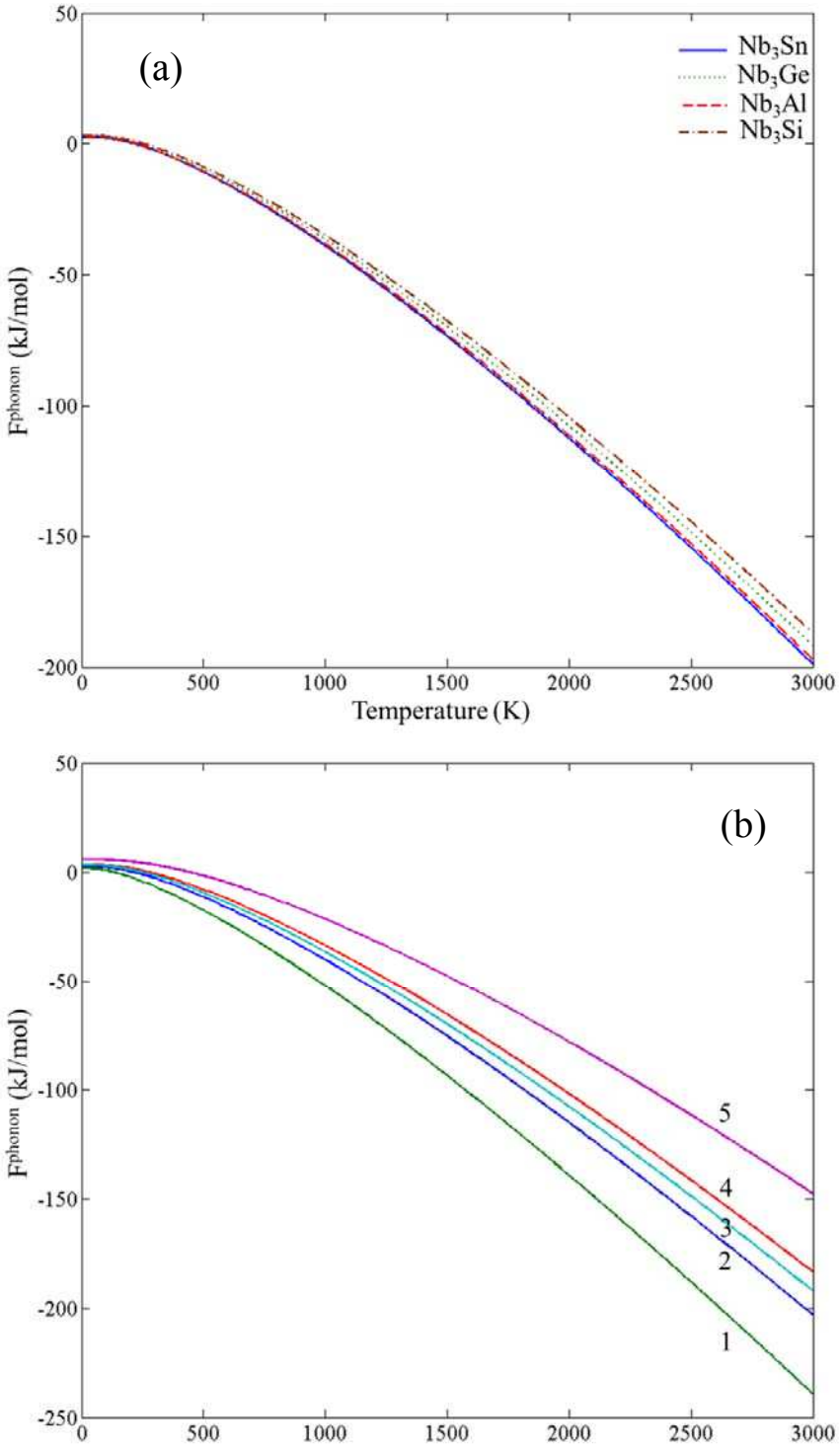

Fig. 2. Phonon contribution to free energies of the (a) binary A15 phases and (b) Sn (1), Nb (2), Ge (3), Al (4) and (5) Si.

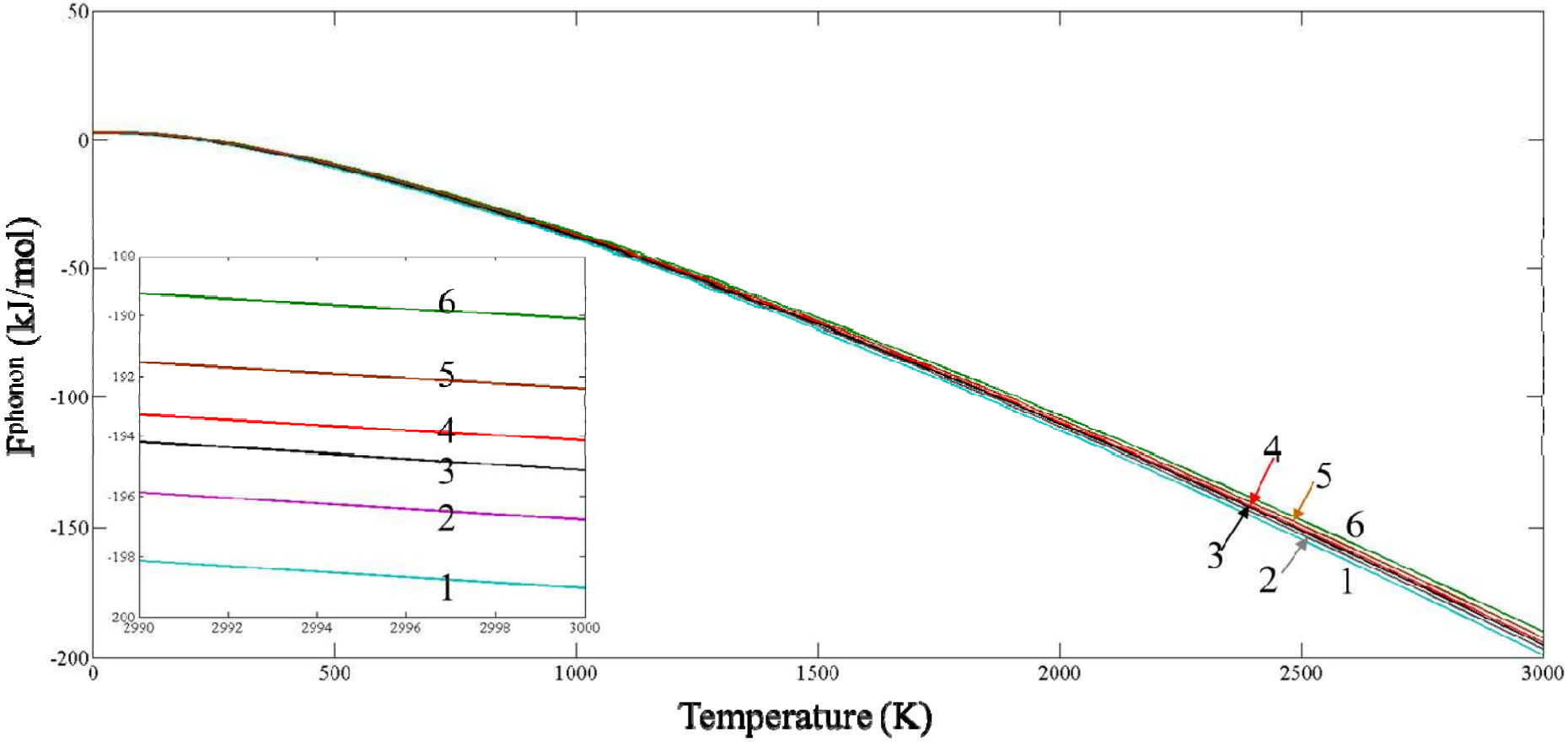

Fig. 3. Phonon contribution to free energies of the ternary A15 phases; Nb_6GeSn (1), Nb_6AlSn (2), Nb_6GeAl (3), Nb_6SiSn (4), Nb_6GeSi (5) and Nb_6AlSi (6).

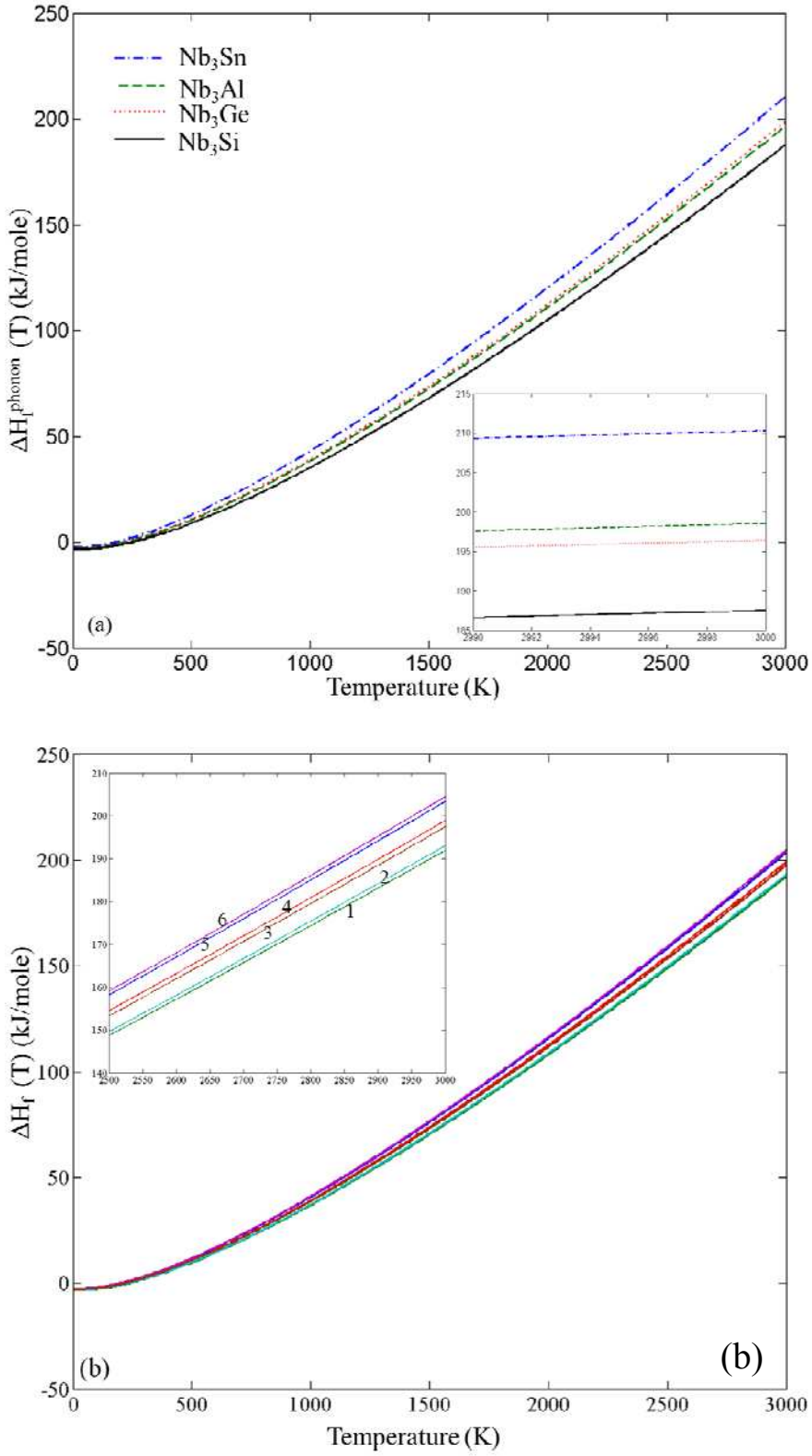

Fig. 4. Phonon contributions to the enthalpy of formation of (a) the binary and (b) the ternary (Nb_6AlSi (1), Nb_6GeSn (2), Nb_6GeAl (3), Nb_6SiSn (4), Nb_6AlSn (5) and Nb_6GeSn (6)) A15 phases.

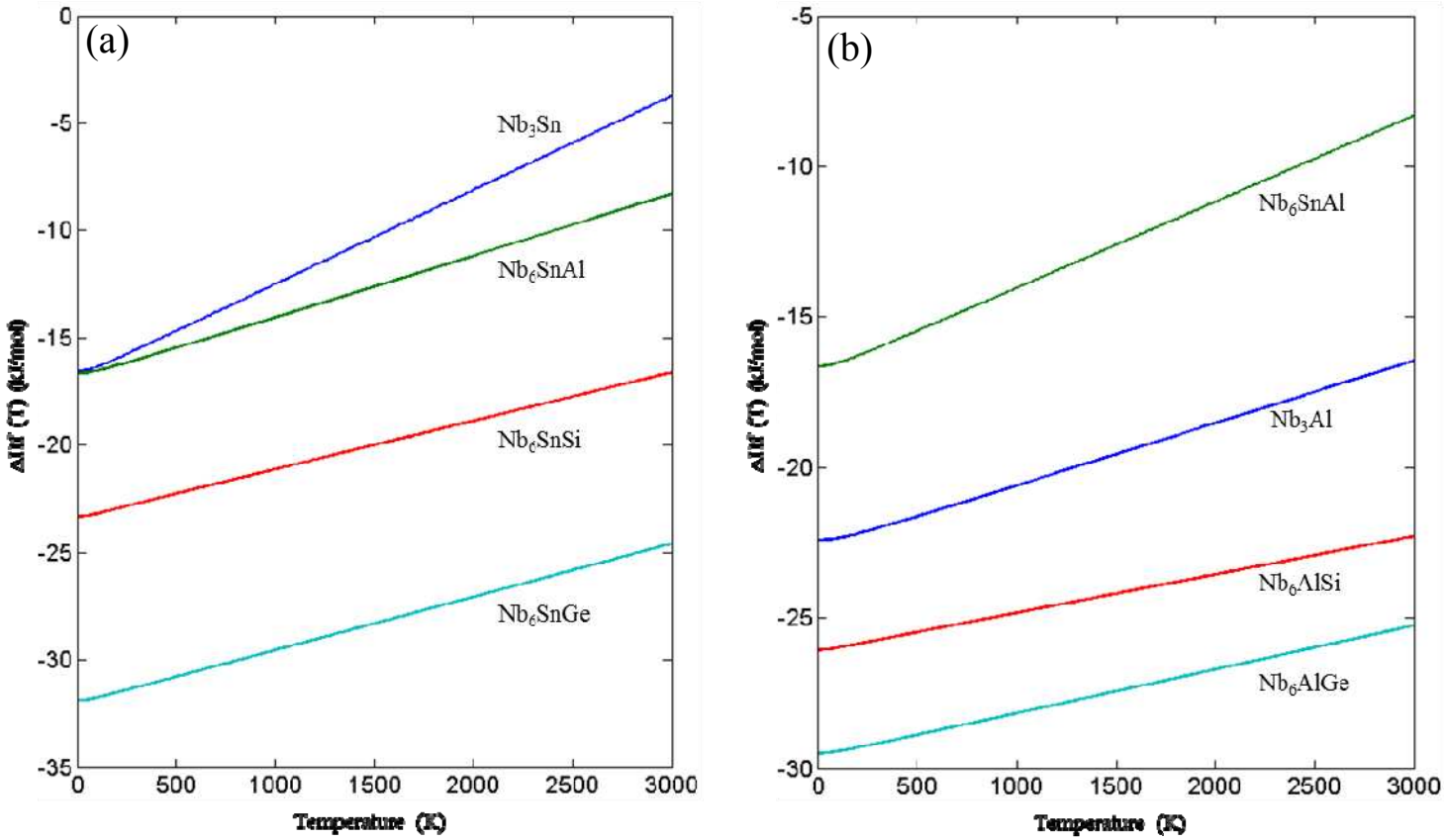

Fig. 5. Enthalpy of formation curves showing the influence of each element under study in the (a) Nb_3Sn and (b) Nb_3Al intermetallics.

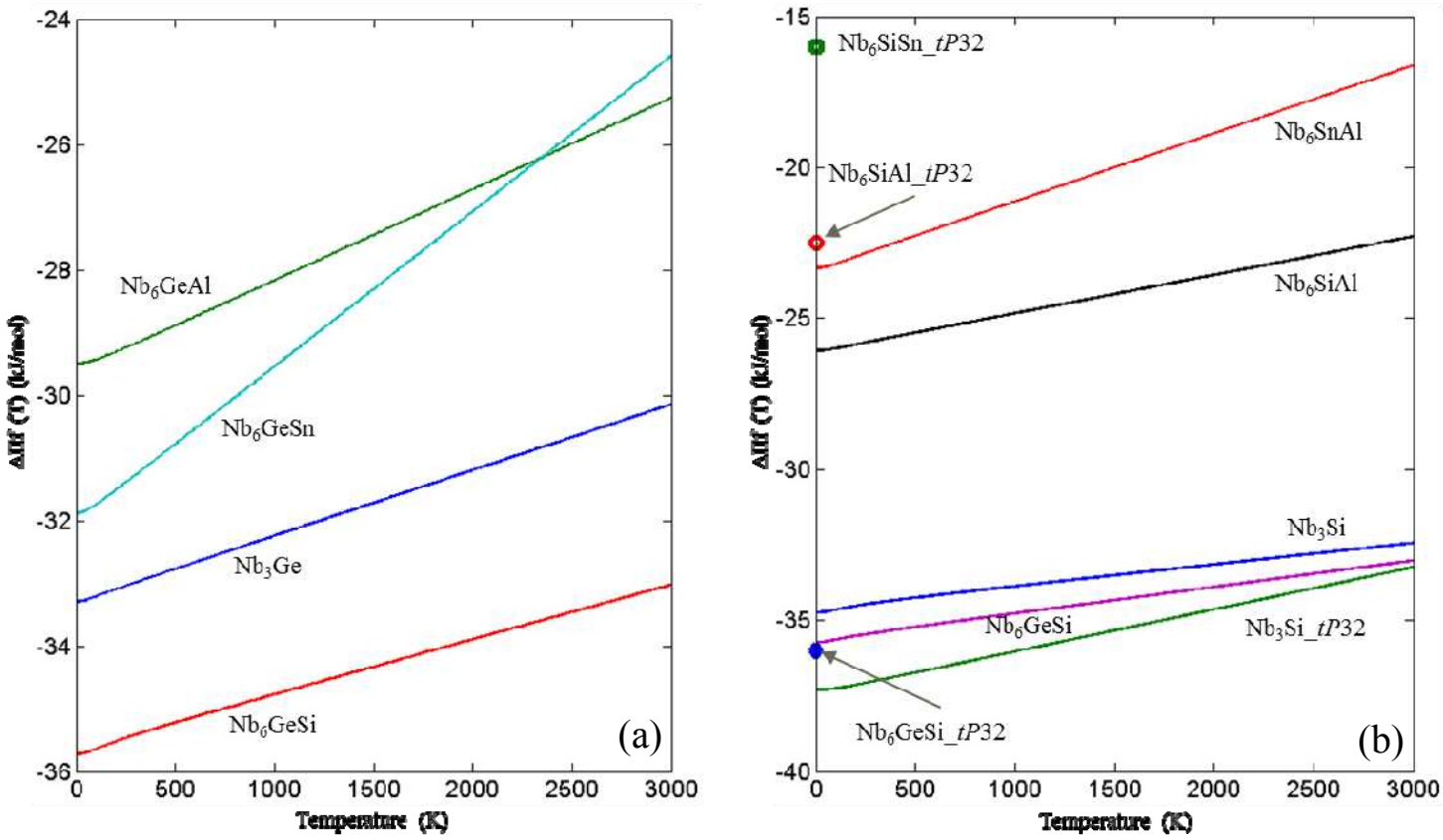

Fig. 6. Enthalpy of formation curves showing the influence of each element under study in the (a) Nb_3Ge and (b) Nb_3Si intermetallics. All phases are of A15 structure unless denoted otherwise.